



Cite this: *Chem. Commun.*, 2015, 51, 12305

Received 30th March 2015,  
Accepted 29th June 2015

DOI: 10.1039/c5cc02623g

www.rsc.org/chemcomm

## Water soluble, cyclometalated Pt(II)–Ln(III) conjugates towards novel bimodal imaging agents†

Oliver J. Stacey,<sup>a</sup> Angelo J. Amoroso,<sup>a</sup> James A. Platts,<sup>a</sup> Peter N. Horton,<sup>b</sup> Simon J. Coles,<sup>b</sup> David Lloyd,<sup>c</sup> Catrin F. Williams,<sup>c</sup> Anthony J. Hayes,<sup>c</sup> Jay J. Dunsford<sup>d</sup> and Simon J. A. Pope\*<sup>a</sup>

**Facile conjugation of a luminescent cyclometalated Pt<sup>II</sup> complex with a DO3A-derived Gd<sup>III</sup> moiety yields a hybrid species with visible luminescence and enhanced relaxivity.**

A number of imaging techniques (MRI, CT, ultrasound, PET, SPECT, optical) are available at a biomedical level with various pros and cons for each regarding image resolution, depth of tissue penetration, acquisition time, and sensitivity. Therefore combining two or more imaging modalities into a single molecule agent can circumvent many limitations associated with a particular technique, whilst simplifying aspects of the agent administration and biodistribution characteristics (pharmacodynamics).<sup>1</sup>

It is very well known that trivalent lanthanide ions (Ln<sup>III</sup>) offer remarkable opportunities in the design of biological imaging agents.<sup>2</sup> With dual applications in optical (luminescence)<sup>3</sup> and magnetic resonance imaging (MRI),<sup>4</sup> Ln<sup>III</sup> complexes have been extensively studied and a range of ligand systems investigated. Therefore Ln<sup>III</sup> moieties are particularly useful as a component of a bi- or multimodal single molecule imaging agent.<sup>5</sup> In this context, systems based on Gd<sup>III</sup> have attracted most attention, with covalent coupling of organic fluorophores (MR/optical),<sup>6</sup> labelling with <sup>18</sup>F (MR/PET)<sup>7</sup> and <sup>99m</sup>Tc chelation (MR/SPECT)<sup>8</sup> providing prospective agents.

We are particularly interested in the use of phosphorescent metal-based luminophores<sup>9</sup> as components of dual MR/optical imaging agents. Such species offer distinct photophysical advantages (tunable emission wavelengths, large Stokes' shifts, long

emission lifetimes) over fluorescent variants and can be very effective in cellular imaging studies using confocal fluorescence microscopy.<sup>10</sup> Cyclometalated Pt<sup>II</sup> complexes can possess many of these beneficial luminescent properties and have been successfully applied to biological imaging.<sup>11</sup> In tandem with such physical attributes, interest in the use of Pt<sup>II</sup> complexes with therapeutic benefits also continues.<sup>12</sup> Indeed one of the challenges of probing the (non)-specific biological action of Pt<sup>II</sup> therapeutics often lies in the difficulty of directly imaging the biological action. In this context, Pt<sup>II</sup> complexes can be tagged with fluorophores, such as anthraquinone, providing a means for identifying the intracellular fate of such compounds and understanding the role of targeting vectors.<sup>13</sup> Recent studies into Pt<sup>II</sup> complexes of 2-phenylpyridine (ppy), have also explored binding with amyloid  $\beta$  peptide.<sup>14</sup> The influences of the Pt complexes on protein aggregation, *via* the inhibition of Cu and Zn peptide complex formation, have been suggested as an approach to the study of Alzheimer's disease.

In this work, we describe the development of water soluble Pt<sup>II</sup>–Ln<sup>III</sup> hybrid systems wherein the cyclometalated Pt<sup>II</sup> moiety is luminescent. Previous work has described the synthesis of mixed Pt<sup>II</sup>/Ln<sup>III</sup> species and their photophysical properties, where the Pt<sup>II</sup> chelate acts as an antenna for sensitised Ln<sup>III</sup> emission within donor (Pt)–acceptor (Ln) assemblies.<sup>15</sup> However, such systems are often not water soluble or water stable, and thus, to the best of our knowledge, there are no reports on the water relaxometric properties of Pt<sup>II</sup>–Gd<sup>III</sup> heterometallic species. A number of other water stable d–f hybrids employing Ru<sup>II</sup>, Re<sup>I</sup> and Os<sup>II</sup> as MLCT-based sensitisers have also been reported,<sup>16</sup> with Re<sup>I</sup>/Ru<sup>II</sup>–Gd<sup>III</sup> hybrids demonstrating the physical properties for potential in dual MR/optical imaging.<sup>17</sup> The aim of this work was to synthesise a water-soluble Pt<sup>II</sup>–Ln<sup>III</sup> complex with favourable luminescence and relaxivity properties.

Two new ligands were required for the assembly of the Pt<sup>II</sup>–Ln<sup>III</sup> targets. Firstly, for the macrocyclic complex (Ln–py), a route was utilised<sup>18</sup> to give the ethylamine amide derivative (P1, ESI†), which subsequently reacted with 4-pyridinecarboxaldehyde using a reductive amination procedure (P2, ESI†);

<sup>a</sup> School of Chemistry, Main Building, Cardiff University, Park Place, Cardiff, UK CF10 3AT. E-mail: pope@cardiff.ac.uk; Tel: +44 02920 879316

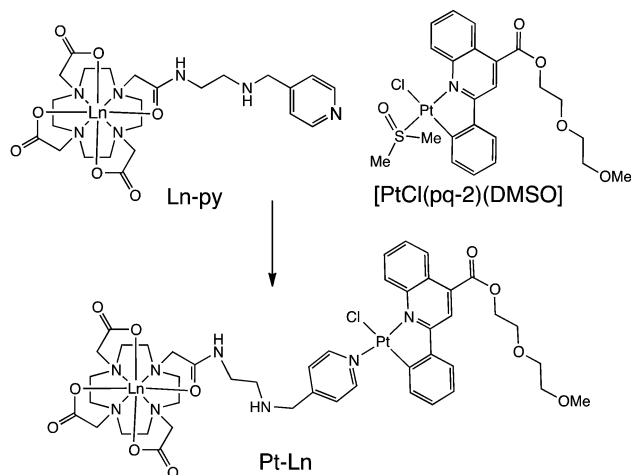
<sup>b</sup> UK National Crystallographic Service, Chemistry, Faculty of Natural and Environmental Sciences, University of Southampton, Highfield, Southampton, UK SO17 1BJ

<sup>c</sup> School of Biosciences, Main Building, Cardiff University, Park Place, Cardiff, UK CF10 3AT

<sup>d</sup> School of Chemistry, The University of Manchester, Manchester, UK M13 9PL

† Electronic supplementary information (ESI) available: All experimental and characterisation details, X-ray crystallographic data, TD-DFT, <sup>1</sup>H NMR spectra and <sup>1</sup>H NMRD plots. CCDC 1056166. For ESI and crystallographic data in CIF or other electronic format see DOI: 10.1039/c5cc02623g



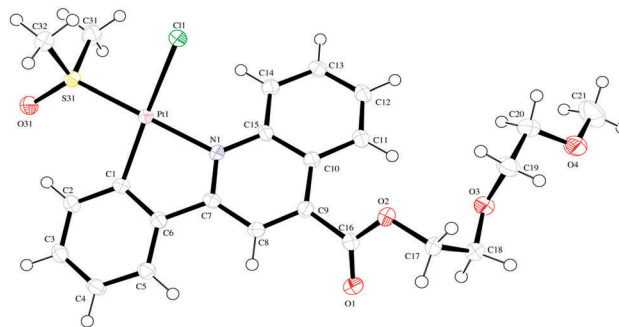


Scheme 1 Route to the heterometallic targets.

deprotection of the *tert*-butyl esters with trifluoroacetic acid and complexation with either  $\text{Gd}(\text{OTf})_3$  or  $\text{Yb}(\text{OTf})_3$  gave the monometallic  $\text{Ln}^{\text{III}}$  complexes, **Ln-py** (Scheme 1) possessing a pendant pyridine donor. Formation of the lanthanide complexes was confirmed by HRMS with additional  $^1\text{H}$  NMR data for **Yb-py** (ESI,† Fig. S1) showing the pronounced chemical shifts of the azamacrocycle and arm protons between +135 and –80 ppm. For the hydrophilic  $\text{Pt}^{\text{II}}$  component, two 2-phenylquinoline derivatives incorporating a PEG-like functionality were synthesised, yielding both amide (**pq-1**, ESI†) and ester linked (**pq-2**, ESI†) derivatives from either 2-(2-aminoethoxy)ethanol or 2-(2-methoxyethoxy)ethanol, respectively.

The attempted synthesis of the  $\text{Pt}^{\text{II}}$  complexes was undertaken *via* the splitting of dimeric  $[(\text{L})\text{Pt}(\mu\text{-Cl}_2)\text{Pt}(\text{L})]$  with DMSO to form the monometallic species  $[\text{PtCl}(\text{pq})(\text{DMSO})]$ . In our hands, the use of the hydroxyl terminated PEG derivative (**pq-1**) was not amenable to this synthetic pathway, giving a poor yield of the desired  $\text{Pt}^{\text{II}}$  complex. However, the methoxy analogue  $[\text{PtCl}(\text{pq-2})(\text{DMSO})]$ , which would be expected to be slightly less hydrophilic than **pq-1**, was successfully isolated as an orange solid suggesting that the terminal hydroxyl group of **pq-1** may interfere with the coordination chemistry of  $\text{Pt}^{\text{II}}$ .  $[\text{PtCl}(\text{pq-2})(\text{DMSO})]$  was characterised *via* a range of techniques including  $^{195}\text{Pt}\{^1\text{H}\}$  NMR which revealed a resonance at –3665 ppm. An X-ray crystal structure (Fig. 1) of  $[\text{PtCl}(\text{pq-2})(\text{DMSO})]$  was also obtained (crystal structure data and refinement parameters are contained in the ESI†) and revealed the anticipated coordination environment for  $\text{Pt}^{\text{II}}$ , with typical Pt–L bond lengths and angles for the coordinated atoms (ESI,† Table S1) and a distortion of *ca.*  $7^\circ$  in the phenylquinoline unit. The packing structure also revealed a head-to-toe arrangement, with some  $\pi$ -stacking between the phenylquinoline moieties; there are no intermolecular Pt–Pt interactions.

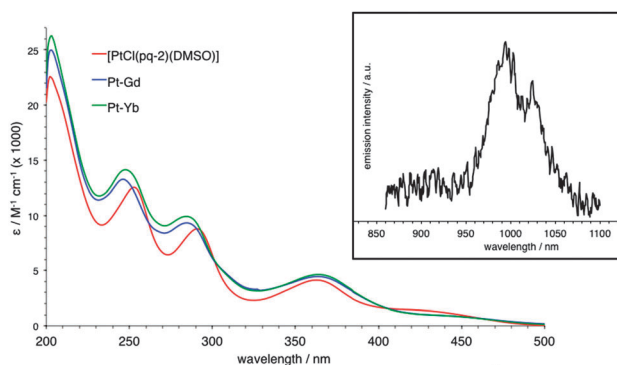
Finally, the two complexes **Ln-py** and  $[\text{PtCl}(\text{pq-2})(\text{DMSO})]$  were dissolved in a minimum volume of acetone and reacted at  $40^\circ\text{C}$  for 48 h. The resultant **Pt-Ln** dimetallic complexes were obtained as extremely hygroscopic orange powders and the formation confirmed using HRMS (ESI,† Fig. S2), which revealed the distinct and appropriate isotopic distribution corresponding

Fig. 1 X-ray crystal structure of  $[\text{PtCl}(\text{pq-2})(\text{DMSO})]$ . Probability of the ellipsoids is 50%.

to the loss of the chloride ligand to give the cationic dimer as  $[\text{M} - \text{Cl}]^+$ .

The electronic properties of  $[\text{PtCl}(\text{pq-2})(\text{DMSO})]$  show that the complex absorbs in the UV region, with  $^1\pi\text{-}\pi^*$  transitions associated with the phenylquinoline unit, and in the visible region with  $\lambda_{\text{max}}$  at 424 nm, which probably corresponds to a  $^1\text{MLCT}$  type transition. Supporting theoretical (TD-DFT) calculations on the model complexes  $[\text{PtCl}(\text{epqc})(\text{DMSO})]$  (where **epqc** = 4-ethyl-2-phenylquinoline carboxylate) and  $[\text{PtCl}(\text{epqc})(\text{py})]$  (where **py** = pyridine) show that the majority of the electron density in the HOMO lies across both the phenyl moiety of the cyclometalated ligand and the 5d-orbitals of the platinum. The orbital representations of the calculated lowest energy HOMO–LUMO transitions are shown in the ESI,† (Fig. S3). The percentage contribution to the energy levels for the  $\text{Pt}^{\text{II}}$  5d-orbitals (ESI,† Table S2) were calculated from the theoretical data showing that for both model complexes the HOMO comprises *ca.* 25% 5d-orbital character and is consistent, therefore, with a MLCT contribution.

The UV-vis spectra (Fig. 2) of the **Pt-Ln** hybrids are closely comparable to  $[\text{PtCl}(\text{pq-2})(\text{DMSO})]$ , with the visible MLCT absorption characteristics retained for both **Pt-Gd** and **Pt-Yb**. The luminescence properties of  $[\text{PtCl}(\text{pq-2})(\text{DMSO})]$  revealed a broad, featureless emission band at 625 nm ( $\lambda_{\text{ex}} = 425$  nm) with a corresponding lifetime of 116 ns, which are attributed to an excited state of triplet character which is likely to encompass a strong  $^3\text{MLCT}$  component. The properties of the corresponding

Fig. 2 Main: UV-vis absorption spectra of the complexes. Inset: Near-IR emission spectrum of **Pt-Yb** recorded in  $\text{D}_2\text{O}$  ( $\lambda_{\text{ex}} = 425$  nm).



- 17 T. Koullourou, L. S. Natrajan, H. Bhavsar, S. J. A. Pope, J. Feng, J. Narvainen, R. Shaw, E. Scales, R. Kauppinen, A. M. Kenwright and S. Faulkner, *J. Am. Chem. Soc.*, 2008, **130**, 2178; G. Dehaen, P. Verwilt, S. V. Eliseeva, S. Laurent, L. V. Elst, R. N. Muller, W. M. De Borggraeve, K. Binnemans and T. N. Parac-Vogt, *Inorg. Chem.*, 2011, **50**, 10005.
- 18 S. G. Crich, D. Alberti, I. Szabo, S. Aime and K. Djanashvili, *Angew. Chem., Int. Ed.*, 2013, **52**, 1161; J. P. Andre, C. Geraldès, J. A. Martins, A. E. Merbach, M. I. M. Prata, A. C. Santos, J. J. P. de Lima and E. Toth, *Chem. – Eur. J.*, 2004, **10**, 5804.
- 19 T. K. Ronson, T. Lazarides, H. Adams, S. J. A. Pope, D. Sykes, S. Faulkner, S. J. Coles, M. B. Hursthouse, W. Clegg, R. W. Harrington and M. D. Ward, *Chem. – Eur. J.*, 2006, **12**, 9299.
- 20 A. Beeby, I. M. Clarkson, R. S. Dickins, S. Faulkner, D. Parker, L. Royle, A. S. de Sousa, J. A. G. Williams and M. Woods, *J. Chem. Soc., Perkin Trans. 2*, 1999, 493.
- 21 J. E. Jones, R. L. Jenkins, R. S. Hicks, A. J. Hallett and S. J. A. Pope, *Dalton Trans.*, 2012, **41**, 10372.
- 22 J. Costa, E. Toth, L. Helm and A. E. Merbach, *Inorg. Chem.*, 2005, **44**, 4747.
- 23 S. J. Coles and P. A. Gale, *Chem. Sci.*, 2012, **3**, 683.

